

Spin Dynamics in Stripe-Ordered $\text{La}_{5/3}\text{Sr}_{1/3}\text{NiO}_4$

A.T. Boothroyd,^{1,*} D. Prabhakaran,¹ P.G. Freeman,¹ S.J.S. Lister,^{1,†} M. Enderle,² A. Hiess,² and J. Kulda²

¹ *Department of Physics, Oxford University, Oxford, OX1 3PU, United Kingdom*

² *Institut Laue-Langevin, BP 156, 38042 Grenoble Cedex 9, France*

(Dated: October 29, 2018)

Polarized and unpolarized neutron inelastic scattering has been used to measure the spin excitations in the spin-charge-ordered stripe phase of $\text{La}_{5/3}\text{Sr}_{1/3}\text{NiO}_4$. At high energies, sharp magnetic modes are observed characteristic of a static stripe lattice. The energy spectrum is described well by a linear spin wave model with intra- and inter-stripe exchange interactions between neighbouring Ni spins given by $J = 15 \pm 1.5$ meV and $J' = 7.5 \pm 1.5$ meV respectively. A pronounced broadening of the magnetic fluctuations in a band between 10 meV and 25 meV is suggestive of coupling to collective motions of the stripe domain walls.

Over the past decade, the tendency of doped antiferromagnetic oxides to exhibit symmetry-broken phases involving the ordering of both spin and charge has become increasingly apparent. Widespread interest was generated by the discovery of a stripe-like, spin-charge ordered phase in a non-superconducting layered cuprate [1]. This stripe phase, the like of which has now been found in many other doped transition metal oxide systems, is characterized by parallel lines of holes that act as charged domain walls separating regions of antiferromagnetically-ordered spins. Its discovery fuelled a debate about the role played by stripe correlations in the formation of the superconducting state in the cuprates [2], and stimulated numerous experimental investigations into stripe phenomena. These have focussed principally on the $\text{La}_{2-x}\text{Sr}_x\text{NiO}_{4+\delta}$ series, which exhibits stripe ordering over a wide range of hole concentration [3, 4].

While the static properties of ordered stripe phases are now quite well characterized, less is known about their dynamics. Specifically, there is a lack of information on how the collective motions of the holes in a stripe domain wall couple to the spin dynamics of the antiferromagnetic domains. One way to make progress in understanding stripe dynamics is to use neutron inelastic scattering to probe the spin excitation spectrum as a function of wavevector and energy in simple compounds exhibiting well-correlated stripe ordering. As well as providing information on the microscopic interactions that govern the properties of stripes, such studies can address the question of whether stripes are essential or incidental to the mechanism of superconductivity.

Here we report polarized- and unpolarized-neutron scattering measurements of the spin excitation spectrum in the ordered stripe phase of $\text{La}_{5/3}\text{Sr}_{1/3}\text{NiO}_4$. This composition has not been studied before by neutron inelastic scattering, and was chosen because the spin-charge order is particularly well correlated and has a very simple superstructure commensurate with the crystal lattice [4, 7, 8, 9] — see Fig. 1(a). Compared with earlier neutron scattering studies of stripe-ordered $\text{La}_{2-x}\text{Sr}_x\text{NiO}_{4+\delta}$ compounds [5, 6] our measurements cover a wider range of wavevector and energy than previously explored in any

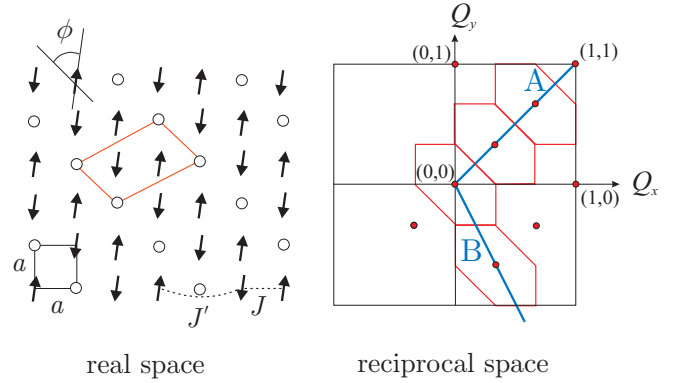


FIG. 1: (a) Model for the stripe order found in the Ni-O plane of $\text{La}_{5/3}\text{Sr}_{1/3}\text{NiO}_4$ [4, 9]. Arrows denote $S = 1$ spins on the Ni^{2+} sites, open circles represent Ni^{3+} holes. The O sites are not shown. ϕ is the angle between the spin axes and the stripe direction. Primitive unit cells of the NiO_2 square lattice and stripe superstructure are indicated respectively by the small square and parallelogram. J and J' are respectively the intra- and inter-stripe exchange interactions between nearest-neighbour Ni spins. (b) Diagram of reciprocal space showing several Brillouin zones for the stripe-order superlattice shown in (a). The (h,k) indices correspond to the NiO_2 square lattice, and the small circles are the stripe superlattice zone centres. The lines marked A and B indicate the directions of the scans used in the experiment.

one compound, and the simplicity of the magnetic structure of $\text{La}_{5/3}\text{Sr}_{1/3}\text{NiO}_4$ allows us to perform a quantitative analysis of the data by linear spin-wave theory. Thus, for the first time in a stripe-ordered compound, we determine values for the nearest-neighbour coupling strengths for spins within a stripe domain and for spins separated by a charged domain wall. We also observe an anomaly in the magnetic scattering between 10 meV and 25 meV that could, we suggest, originate from coupling between spin excitations and collective motions of the charged domain walls.

Two single crystals of $\text{La}_{5/3}\text{Sr}_{1/3}\text{NiO}_4$ in the form of rods, 7–8 mm in diameter and ~ 40 mm in length, were used for the experiments. Both were grown from

the same batch of starting powder by the floating-zone method [10]. Their oxygen excess was determined by thermogravimetric analysis to be $\delta = 0.01 \pm 0.01$, and their electrical and magnetic properties were found to be in very good agreement with data in the literature.

Neutron inelastic scattering measurements were performed on the IN20 and IN22 triple-axis spectrometers at the Institut Laue-Langevin. The incident and final neutron energy was selected by Bragg reflection from an array of either pyrolytic graphite (PG) or Heusler alloy crystals, depending on whether unpolarized or polarized neutrons were employed. Scans were performed with a fixed final energy of either $E_f = 14.7$ meV or 34.8 meV, and a PG filter was present to suppress higher-order harmonics in the scattered beam. Two settings of the crystal were used, giving access to the (h, h, l) and $(h, -2h, l)$ planes in reciprocal space. In this paper the reciprocal lattice is indexed with respect to a body-centred tetragonal lattice with cell parameters $a = 3.8$ Å and $c = 12.7$ Å.

Long-range ordering of holes and spins in $\text{La}_{5/3}\text{Sr}_{1/3}\text{NiO}_4$ occurs below $T_{\text{CO}} \simeq 240$ K and $T_{\text{SO}} \simeq 200$ K respectively. The stripe arrangement formed in the Ni-O layers is shown in Fig. 1(a) [4, 9]. In this model the spins are collinear, and ϕ is the angle between the spin axes and the stripe direction. All the measurements reported here were taken at $T = 14$ K, at which temperature $\phi = 53^\circ$ [9] and the in-plane and out-of-plane spin and charge order correlation lengths are several hundred Å and 20–50 Å respectively [4, 8]. In inelastic measurements the c axis correlations were found to decay very rapidly with energy, entirely disappearing above 5 meV. Over the energy range considered here it is therefore reasonable to treat the spin dynamics as two-dimensional.

Fig. 1(b) shows several two-dimensional Brillouin zones of the stripe order. We probed the excitation spectrum either by scanning the neutron scattering vector \mathbf{Q} along the lines marked A and B at a fixed energy, or by scanning the energy at a fixed \mathbf{Q} . In reality, the ordered stripe phase contains equal proportions of two twins with stripes at 90° to one another. The reciprocal space for the second twin is rotated by 90° with respect to that shown in Fig. 1(b). Experimentally, one observes a superposition of the scattering from both twins.

Assuming the ordered ground state in Fig. 1 one expects to observe magnetic excitations dispersing from the magnetic zone centres, and indeed this is confirmed by our measurements. To illustrate the results, Fig. 2 shows wavevector scans parallel to the $(h, h, 0)$ and $(h, -2h, 0)$ directions measured with unpolarized neutrons at a fixed energy of 70 meV. The six peaks observed in Fig. 2(a) correspond to spin excitations propagating in a direction perpendicular to the stripes away from successive zone centres along the A line in Fig. 1(b). Similarly, the two strongest peaks in Fig. 2(b) are spin excitations propagating away from $(1/3, -2/3)$ along line B, approximately

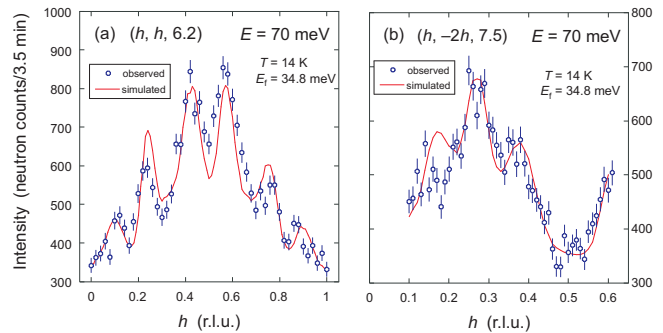


FIG. 2: \mathbf{Q} scans parallel to (a) $(h, h, 0)$ and (b) $(h, -2h, 0)$ at a constant energy of 70 meV, showing the magnetic scattering from $\text{La}_{5/3}\text{Sr}_{1/3}\text{NiO}_4$. The lines are simulations of the scans generated by convolution of the calculated spectrometer resolution with the spin-wave model discussed in the text.

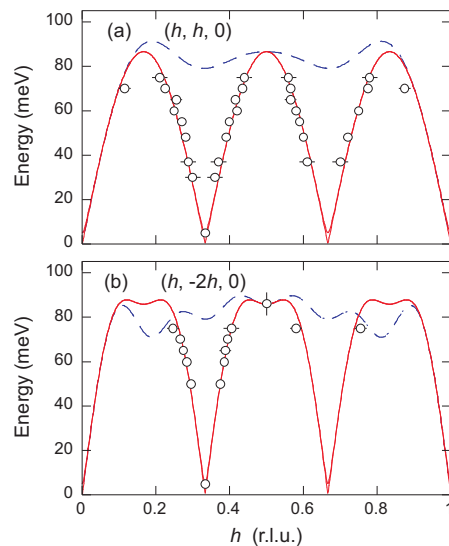


FIG. 3: Dispersion of the magnetic excitations in $\text{La}_{5/3}\text{Sr}_{1/3}\text{NiO}_4$ parallel to (a) $(h, h, 0)$ and (b) $(h, -2h, 0)$. The full and broken lines are the spin-wave model dispersion for the two twins, calculated with parameters $J = 15$ meV, $J' = 7.5$ meV, and $K_c = 0.07$ meV.

parallel to the stripes. Under the experimental conditions used we were not able to resolve the separate peaks associated with each zone centre when the energy was below 37 meV.

In Figs. 3 we plot the dispersion of the spin excitations along the $(h, h, 0)$ and $(h, -2h, 0)$ directions as deduced from a series of (mainly) constant-energy scans like those of Figs. 2. To arrive at the data points shown in Figs. 3 we corrected the observed peak positions for small shifts (10–20%) caused by the spectrometer resolution as it intersects the curved dispersion surface. We determined the corrections by convolution of the resolution function with the model dispersion surface to be described later.

In the energy range 10–30 meV very strong scattering from phonons makes it difficult to identify unam-

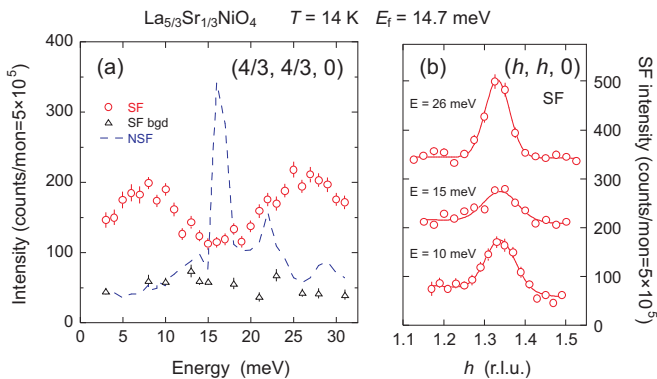


FIG. 4: (a) Spin-flip (SF) and non-spin-flip (NSF) scattering as a function of energy at a constant wavevector of $(4/3, 4/3, 0)$. The sharp peaks in the NSF channel are due to phonons. The SF background is estimated from data collected at $(1.2, 1.2, 0)$. (b) SF scattering intensity plotted as a function of wavevector for energies of 10 meV, 15 meV and 26 meV. The upper two scans have been shifted vertically by 150 and 300 counts respectively. The lines are fits to Gaussian peak profiles. A monitor of 5×10^5 corresponds to a counting time of 5–8 mins, depending on energy.

biguously the magnetic scattering with unpolarized neutrons. Therefore, to explore this energy range we employed polarization analysis, keeping the neutron polarization direction \mathbf{P} parallel to \mathbf{Q} by adjusting currents in a Helmholtz coil mounted around the sample position. In this configuration the neutron spins are flipped when scattered by magnetic excitations, but remain unchanged in non-magnetic (e.g. phonon) scattering processes.

Fig. 4(a) shows the neutron spin-flip (SF) and non-spin-flip (NSF) scattering observed as a function of energy with \mathbf{Q} fixed at the $(4/3, 4/3, 0)$ magnetic zone centre. The separation of the magnetic and non-magnetic scattering by the polarization analysis is exemplified by the sharp phonon peaks centred on 16.5 meV and 22 meV in the NSF channel that are not present in the SF channel. However, the most remarkable feature in this scan is the broad valley centred near 15 meV in the SF scattering. By comparison with the SF measurements made at $\mathbf{Q} = (1.2, 1.2, 0)$, where the magnetic scattering has decreased to background level, we see that the amplitude of the magnetic signal above background is nearly a factor 3 smaller at $E = 15$ meV than at either $E = 10$ meV or $E = 26$ meV. Similar scans measured at $(1/3, 1/3, l)$, $l = 4.5, 5.5$, show the same valley feature. A secondary feature in Fig. 4(a) is the fall in magnetic intensity with energy observed below ~ 7 meV.

One possible origin for the features just described could be spin anisotropy gaps in the excitation spectrum. Below an anisotropy gap a component of the spin fluctuations freezes out, causing a reduction in scattering intensity. We checked this possibility by comparing the magnetic scattering intensities for neutron polarizations

$\mathbf{P} \parallel \mathbf{Q}$ and $\mathbf{P} \perp \mathbf{Q}$. The data at 10 meV, 15 meV and 26 meV were all consistent with the assumption of isotropic transverse spin fluctuations about the direction of the ordered moment. At 3 meV, however, the signal is predominantly due to in-plane transverse spin fluctuations. Therefore, we conclude that the drop in intensity below ~ 7 meV is caused by an out-of-plane anisotropy gap, but that the main valley feature cannot be explained by spin anisotropy.

Fig. 4(b) shows the SF scattering intensity measured in a series of constant-energy scans in the neighbourhood of the valley feature. These data show that, in addition to a reduction in amplitude, there is also an increase in width. The 15 meV peak is found to be $\sim 50\%$ broader in wavevector than the 10 meV and 26 meV peaks. This broadening suggests that the valley feature is associated with the decay of antiferromagnetic spin excitation modes through hybridisation with another type of excitation. One possibility is a coupling to optic phonons intrinsic to the material, but we do not believe this to be the case because (a) the valley region is ~ 10 meV wide, much larger than the width of individual phonon excitations, and (b) we do not observe any structure in the SF scattering channel due to the excitation of phonons through a magnetoelastic interaction. Instead, we suggest that a probable explanation for the valley feature is the interaction between spin excitations and motions of the stripe domain walls with characteristic frequencies in the 3–5 THz range.

Having established the overall features of the spin excitation spectrum we now describe the spin-wave model used to extract the microscopic exchange parameters. The model is based on the spin Hamiltonian

$$H = J \sum_{\langle ij \rangle_{\text{intra-stripe}}} \mathbf{S}_i \cdot \mathbf{S}_j + J' \sum_{\langle ij' \rangle_{\text{inter-stripe}}} \mathbf{S}_i \cdot \mathbf{S}_{j'} + K_c \sum_i (S_i^z)^2, \quad (1)$$

where the first two summations are over pairs of nearest-neighbouring Ni spins, the first sum having both spins within the same stripe domain and the second having the two spins in adjacent domains separated by a line of holes. J and J' are the corresponding exchange parameters — see Fig. 1(a). The third term describes the out-of-plane anisotropy. The in-plane anisotropy is much smaller than the out-of-plane anisotropy, and so is neglected.

We calculated the energy dispersion and scattering cross-section using the linear spin-wave approximation, and after convolving the model spectrum with the spectrometer resolution we compared the results with the measured scans. The parameter values giving the best agreement with the totality of data are $J = 15 \pm 1.5$ meV, $J' = 7.5 \pm 1.5$ meV and $K_c = 0.07 \pm 0.01$ meV. For reference, the J and K_c parameters obtained by Nakajima *et al* [11] from a fit to the spin-wave dispersion of La_2NiO_4 were 15.5 meV and 0.52 meV respectively. We

find, therefore, that the spin anisotropy is strongly reduced in the doped compound, but the strength of the nearest-neighbour exchange interaction in the antiferromagnetic region is essentially unaffected by hole-doping.

The lines drawn on Figs. 2(a) and (b) illustrate scan simulations, and are seen to match the main features of the data quite well. The inclusion of more exchange parameters might achieve even better agreement with experiment, but is not justified given the extent of the present data set. We did, however, consider an alternative model in which J' couples pairs of spins displaced by (a, a) across a domain wall instead of $(2a, 0)$. However, the deviations from the first model were slight and mainly confined to energies close to the zone boundary energy where the data is sparse. Therefore, while there may be systematic errors due to the linear approximation and the neglect of more distant couplings, we expect that the present analysis yields a good estimate of the relative strengths of the intra- and inter-stripe spin couplings.

The results presented here provide several new insights into the dynamics of stripe phases. At high energies ($\gtrsim 30$ meV) the spin excitations propagate as if the underlying charge-ordered lattice were static. A similar observation has been made by Bourges *et al* [6], who also commented on a lack of significant anisotropy in the spin-wave velocity in their study of $\text{La}_{0.169}\text{Sr}_{0.31}\text{NiO}_4$. The advantage of the $\text{La}_{5/3}\text{Sr}_{1/3}\text{NiO}_4$ compound studied here is its simple stripe superstructure that permits us to quantify the anisotropy in the spin-wave dispersion in terms of a microscopic model. Thus, while our data are consistent with those of Bourges *et al*, our analysis has determined the ratio J/J' to be close to 2 and uncovered a dramatic reduction in single-ion spin anisotropy relative to La_2NiO_4 .

Concerning the anomalous broadening observed in the energy range 10–25 meV, we earlier discussed several pieces of evidence that lead us to suggest that this broadening arises from a coupling between spin excitations and the collective motions of the stripe domain walls. Further to these, we note that the stripe ordering temperature (~ 240 K) in this compound translates to ~ 20 meV. In other words, the thermal energy needed to destroy long-range order of the stripes is comparable to the energy where we observe the anomalous broadening in the spin excitations. Zaanen *et al* [12] discussed the dynamics of charged domain wall motion in an antiferromagnetic background on general theoretical grounds, and argued that domain wall fluctuations will have their strongest influence on the spin excitation spectrum at low energies. In one reading this is consistent with our results, but it is interesting that the anomalous broadening appears to be restricted to a band of energies below which the spin excitations recover their sharp profile. A possible explanation is that there exists a commensurability gap of ~ 10 meV for domain wall motions due to the pinning of the charges to the lattice. If this were the case, then

one might expect the valley feature to be absent from the spin excitation spectrum of compounds whose stripe period is incommensurate with the lattice.

Finally, we draw attention to recent calculations of the imaginary parts of the charge and spin dynamical susceptibilities of an ordered stripe system described by the Hubbard model [13, 14]. In addition to transverse spin waves these calculations also predict longitudinal modes arising from meandering and compressive movements of the domain walls. We did not observe sharp phason-like modes of the type predicted, but their weak intensity relative to the spin wave scattering and the broadening in the valley region may have precluded their observation. Similar calculations for the special case of $1/3$ doping, incorporating the experimentally-determined exchange parameters, would be valuable for interpreting the features we have measured, and would thus provide a direct test of this theoretical description of stripe dynamics.

We thank L.-P. Regnault for help with the IN22 experiments, P. Isla, D. Gonzalez and R. Burriel for sample characterization, and J. Zaanen and J. Chalker for stimulating discussions. ATB is grateful to the Institut Laue-Langevin for support during a 3-month visit in 2002. This work was supported by the Engineering & Physical Sciences Research Council of Great Britain.

* Electronic address: a.boothroyd1@physics.ox.ac.uk;
URL: <http://xray.physics.ox.ac.uk/Boothroyd>

† Present address: Oxford Magnet Technology Ltd, Witney, Oxfordshire, OX29 4BP, United Kingdom

- [1] J. M. Tranquada *et al*, Nature **375**, 561 (1995).
- [2] J. Zaanen and O. Gunnarsson, Phys. Rev. B **40**, 7391 (1989); V. J. Emery and S. A. Kivelson, Physica (Amsterdam) **209C**, 597 (1993); J. Zaanen, Nature **404**, 714 (2000).
- [3] C. H. Chen, S.-W. Cheong, and A. S. Cooper, Phys. Rev. Lett. **71**, 2461 (1993); J. M. Tranquada *et al*, Phys. Rev. Lett. **73**, 1003 (1994).
- [4] H. Yoshizawa *et al*, Phys. Rev. B **61**, R854 (2000).
- [5] S. M. Hayden *et al*, Phys. Rev. Lett. **68**, 1061 (1992); J. M. Tranquada, P. Wochner, and D. J. Buttrey, Phys. Rev. Lett. **79**, 2133 (1997); K. Nakajima and Y. Endoh, J. Phys. Soc. Jpn. **67**, 1552 (1998); S.-H. Lee *et al*, Phys. Rev. Lett. **88**, 126401 (2002).
- [6] P. Bourges *et al*, cond-mat/0203187.
- [7] S.-W. Cheong *et al*, Phys. Rev. B **49**, 7088 (1994).
- [8] C.-H. Du *et al*, Phys. Rev. Lett. **84**, 3911 (2000).
- [9] S.-H. Lee *et al*, Phys. Rev. B **63**, 060405 (2001).
- [10] D. Prabhakaran, P. Isla, and A. T. Boothroyd, to be published in J. Cryst. Growth (2002).
- [11] K. Nakajima *et al* J. Phys. Soc. Jpn. **62**, 4438 (1993).
- [12] J. Zaanen *et al*, Phys. Rev. B **53**, 8671 (1996).
- [13] E. Kaneshita, M. Ichioka, and K. Machida, J. Phys. Soc. Jpn. **70**, 866 (2001), and cond-mat/0005466.
- [14] S. Varlamov and G. Seibold, Phys. Rev. B **65**, 075109 (2002).